



**Discover Generics**

Cost-Effective CT & MRI Contrast Agents

 **FRESENIUS  
KABI**

[WATCH VIDEO](#)

**AJNR**

**Hemorrhagic Neoplasms: MR Mimics of Occult Vascular Malformations**

Gordon Sze, George Krol, Walter L. Olsen, Paul S. Harper, Joseph H. Galicich, Linda A. Heier, Robert D. Zimmerman and Michael D. F. Deck

This information is current as of June 23, 2025.

*AJNR Am J Neuroradiol* 1987, 8 (5) 795-802  
<http://www.ajnr.org/content/8/5/795>

# Hemorrhagic Neoplasms: MR Mimics of Occult Vascular Malformations

Gordon Sze<sup>1,2</sup>  
 George Krol<sup>1</sup>  
 Walter L. Olsen<sup>3</sup>  
 Paul S. Harper<sup>3,4</sup>  
 Joseph H. Galicich<sup>5</sup>  
 Linda A. Heier<sup>2</sup>  
 Robert D. Zimmerman<sup>2</sup>  
 Michael D. F. Deck<sup>2</sup>

The MR scans of 24 patients who had findings previously reported to be characteristic of occult cerebral vascular malformations were reviewed to demonstrate that such findings may also occur in primary or secondary neoplasms. Eighteen of the 24 patients were found to have hemorrhagic neoplasms. Additional criteria, such as multiplicity of lesions and the presence of edema, were of some help in differentiating between occult vascular malformation and hemorrhagic neoplasm. In certain cases, CT was necessary to provide further information, such as the presence of calcification; however, an absolute and accurate diagnosis was impossible in several cases. The striking similarity on MR between cryptic vascular malformation and some hemorrhagic neoplasms is most likely due to the unifying mechanisms that underlie the evolution of extravascular intracerebral blood.

Although the preponderance of neoplastic etiologies in our series may be partly due to the strong bias in our sample population toward patients with tumors, it seems clear that when an MR scan discloses findings "typical" of an occult vascular malformation, consideration must also be given to the generally more serious possibility of underlying neoplasm.

Recently, several reports have appeared that describe the MR appearance of angiographically occult vascular malformation of the brain [1–5]. These lesions typically consist of central foci of high-intensity signal, thought to be most consistent with subacute to chronic hemorrhage, surrounded by a peripheral zone of low intensity, attributed most frequently to the paramagnetic effect of hemosiderin deposition. This characteristic appearance is distinctive and has been described as specific and virtually pathognomonic of cryptic vascular malformation [2, 6].\*

We saw a large number of lesions with the "typical" MR features of angiographically occult vascular malformations; however, by pathologic or clinical criteria, the majority of these abnormalities were found to be hemorrhagic neoplasms. This report describes our experience and suggests certain criteria that may help to specify the actual etiology of lesions that have this appearance on MR.

## Materials and Methods

The MR scans of 24 patients with lesions thought to be consistent with angiographically occult vascular malformations were reviewed. Criteria for inclusion in this study consisted of two patterns:

1. A central cystic focus or foci of isointensity or high-intensity signal on both T1- and T2-weighted images, with peripheral hypointensity surrounding the central focus of signal.
2. A focus of low-intensity signal, fading peripherally, on both T1- and T2-weighted images, less than 1 cm in diameter, without associated foci of isointensity or high intensity.

MR imaging was performed on a superconductive scanner operating at 1.5 T. Each patient received both T1-weighted (TR 600 msec, TE 20 msec), proton density and T2-weighted (TR 2000 msec, TE 35/70 msec) spin-echo pulse sequences, with two excitations. Multislice data acquisition was used to acquire 5-mm-thick slices, separated by a gap of 2.5 mm. The matrix was 256 × 256.

\* The term vascular malformation is used here to include cavernous hemangioma, capillary telangiectasia, arteriovenous malformation, and venous angioma. Of these, cavernous hemangioma fits the pathologic criteria most consistent with the MR appearance [2, 6].

This article appears in the September/October 1987 issue of *AJNR* and the December 1987 issue of *AJR*.

Received December 30, 1986; accepted after revision April 22, 1987.

<sup>1</sup> Department of Medical Imaging, Memorial Sloan-Kettering Cancer Center, 1275 York Ave., New York, NY 10021. Address reprint requests to G. Sze.

<sup>2</sup> Department of Radiology, New York Hospital, 525 E. 68th St., New York, NY 10021.

<sup>3</sup> Department of Radiology, University of California, San Francisco, San Francisco, CA 94143.

<sup>4</sup> Present address: Highlands Diagnostic Center, 2173 Highland Ave., Birmingham, AL 35205.

<sup>5</sup> Department of Neurosurgery, Memorial Sloan-Kettering Cancer Center, 1275 York Ave., New York, NY 10021.

*AJNR* 8:795–802, September/October 1987  
 0195–6108/87/0805–0795

© American Society of Neuroradiology

All patients were also studied with CT. Scans were obtained without and with contrast. In 13 of the 24 patients, there was surgical verification of their lesions. The remaining patients were followed for up to 1½ years, both clinically and with repeat MR and/or CT scans. Ages of the patients ranged from 10–75 years; there were 14 men and 10 women.

Fifteen of the patients had known systemic malignancies at the time of their imaging studies. There were eight cases of melanoma, two of lung carcinoma, two of colon carcinoma, and one case each of breast carcinoma, choriocarcinoma, and metastatic teratoma. None of these patients had a history of cerebral metastasis and none had received prior radiation therapy to the central nervous system. Evaluation was prompted by symptomatology. Headache was the most frequently encountered symptom, with seizures or focal neurologic deficit much less common.

Nine of the patients had no known systemic malignancy. One of these patients was studied as follow-up for known primary glioma. The remaining eight patients had nondescript symptoms consisting of headache or nausea. Two of these also had focal neurologic deficits or seizures.

## Results

Six of the 24 cases proved to be occult vascular malformations. Five of these were demonstrated at surgery. The sixth patient had no clinical or radiologic symptoms during follow-up over the next 1½ years and had no known systemic malignancy or focal sign. This patient's headache also resolved after treatment for migraine.

**TABLE 1: Comparison of CT Appearance of Different Pathologic Entities<sup>a</sup>**

CT Appearance	Cryptic Vascular Malformation (n = 6)	Primary Cerebral Neoplasms (n = 3)	Metastasis (n = 15)
1. Calcification	2/9 lesions 2/6 cases	2/3	0/42 lesions 0/15 cases
2. Hyperdense, without calcification, precontrast	5/9 lesions 3/6 cases	0/3	20/42 lesions 7/15 cases
3. Hypodense, precontrast	1/9 lesions 1/6 cases	2/3	2/42 lesions 1/15 cases
4. Isodense, precontrast	1/9 lesions 1/6 cases	1/3	10/42 lesions 4/15 cases
5. Ring lesion, precontrast	0/9 lesions 0/6 cases	0/3	2/42 lesions 2/15 cases
6. Enhancement	9/9 lesions 6/6 cases	3/3	34/42 lesions 13/15 cases
7. Negative scan	0/9 lesions 0/6 cases	0/3	8/42 lesions 2/15 cases

<sup>a</sup> For cryptic vascular malformation and cerebral metastasis, the number of lesions is listed separately from the number of cases because certain cases contained multiple lesions with different appearances.

**TABLE 2: Comparison of MR Appearance of Different Pathologic Entities<sup>a</sup>**

MR Appearance	Cryptic Vascular Malformation (n = 6)	Primary Cerebral Neoplasm (n = 3)	Cerebral Metastasis (n = 15)
<b>T1 Weighting</b>			
1. Isointense or hyperintense, central focus	8/9 lesions 5/6 cases	3/3	42/42 lesions 15/15 cases
2. Hypointense throughout lesion	1/9 lesions 1/6 cases	0/3	0/42 lesions 0/15 cases
3. Hypointense rim	8/9 lesions 5/6 cases	3/3	38/42 lesions 12/15 cases
<b>T2 Weighting</b>			
1. Isointense or hyperintense, central focus	8/9 lesions 5/6 cases	3/3	42/42 lesions 15/15 cases
2. Hypointense throughout lesion	1/9 lesions 1/6 cases	0/3	0/42 lesions 0/15 cases
3. Hypointense rim	8/9 lesions 5/6 cases	3/3	42/42 lesions 15/15 cases
4. Edema	2/9 lesions 2/6 cases	1/3	35/42 lesions 12/15 cases

<sup>a</sup> For cryptic vascular malformation and cerebral metastasis, the number of lesions is listed separately from the number of cases because certain cases contained multiple lesions with different appearances.

Eighteen of the 24 cases were believed to be hemorrhagic neoplasms. Of these, 10 were proven by surgical pathology. The remaining eight cases were considered valid on the basis of clinical criteria. These eight consisted of patients with known extensive metastases elsewhere from systemic malignancies. The CT and MR findings are summarized in Tables 1 and 2.

#### *Occult Vascular Malformations*

CT scans detected all lesions in the six cases with occult vascular malformations. In two of the six cases, punctate high density was seen on unenhanced CT scans, consistent with calcification (Fig. 1). One case consisted of an isodense lesion on noncontrast CT scans. Three of the six cases contained

lesions that were hyperdense but not definitely calcified. In one of these cases, an additional hypodense lesion was also seen (Fig. 2). In all six cases, contrast enhancement was present. The case with the hypodense lesion showed some peripheral, ill-defined enhancement. In five cases, the lesions were solitary. However, one patient had four cryptic malformations.

MR also detected all lesions in the six cases with occult malformations. In two cases, a central focus of isointensity was present on the T1-weighted images (Fig. 3). In three cases, the central focus was primarily hyperintense. These foci were surrounded by variable areas of low signal. These isointense or hyperintense regions on T1-weighted images acted variably on proton density and T2-weighted images. Some persisted or became more intense while others became

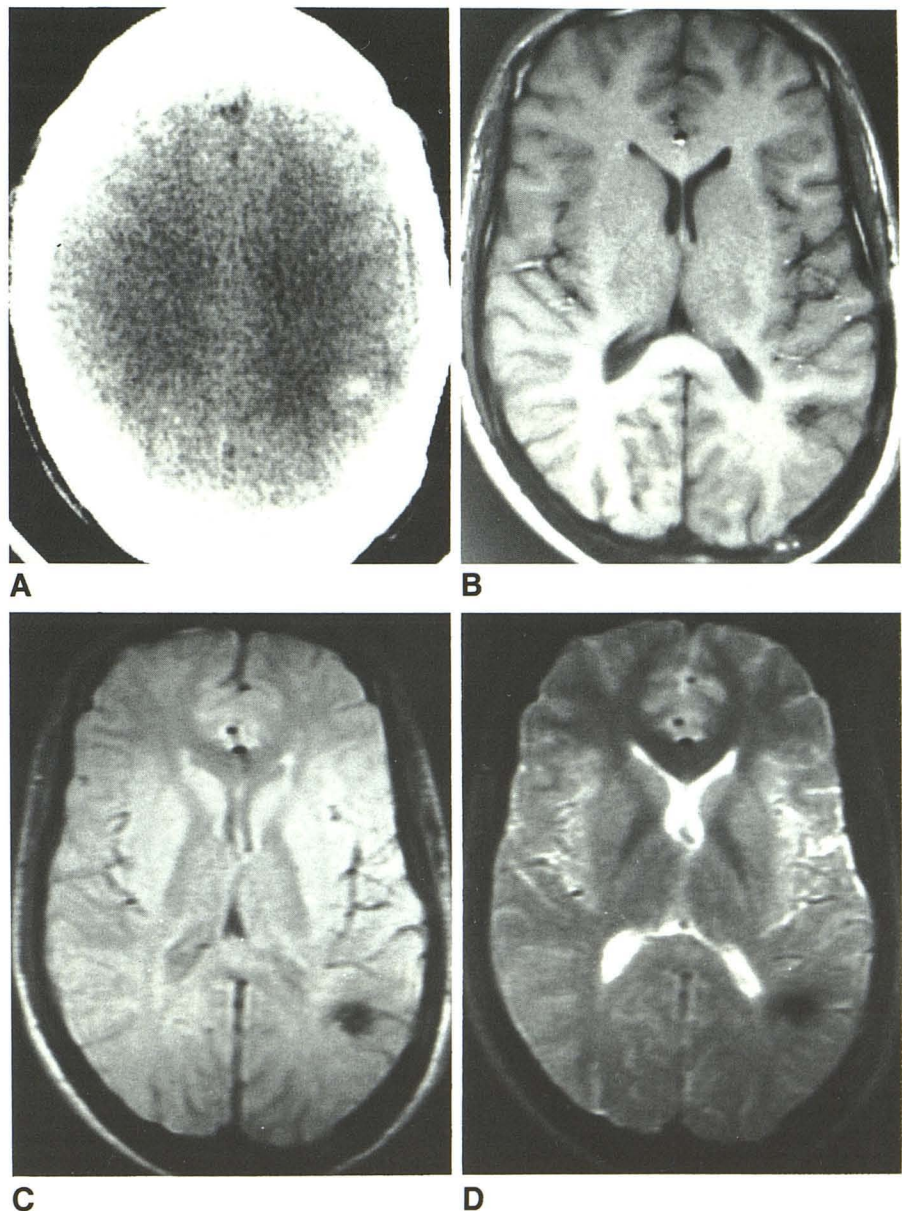


**Fig. 1.**—26-year-old man with headaches. Surgical pathology: cryptic vascular malformation.

**A,** Noncontrast CT scan shows slightly dense lesion, consistent with calcification, in posterior portion of left centrum semiovale. Mild contrast enhancement was seen.

**B,** T1-weighted MR scans (TR 600 msec, TE 25 msec) show a small hypointense lesion.

**C and D,** Proton density and T2-weighted images (TR 2000 msec, TE 35/70 msec) show the lesion to be even more prominent than on T1-weighted images. Part of the low intensity is due to calcification, confirmed by the CT scan. However, that the lesion becomes even more hypointense on the T2-weighted image suggests a significant contribution of hemosiderin effect.

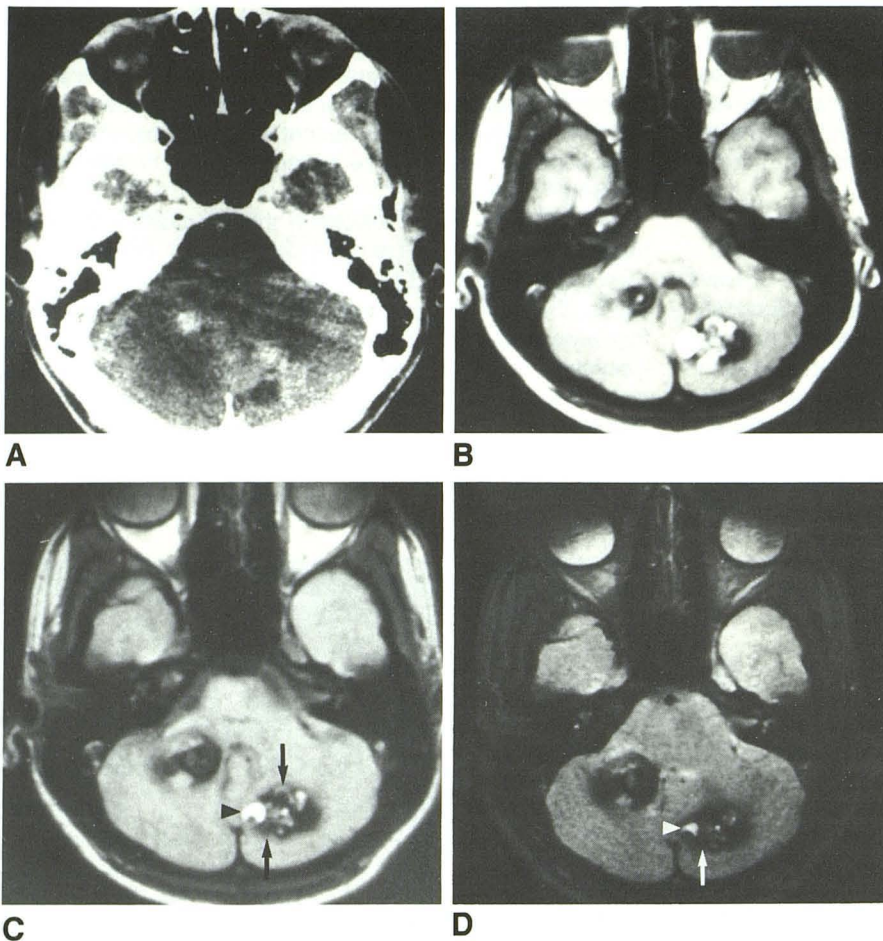


Fig. 2.—22-year-old woman with ataxia. Surgical pathology: cryptic vascular malformation.

A, Contrast-enhanced CT scan shows an enhancing focus in right cerebellum with a hypodense focus in left cerebellum. There may be a small amount of associated peripheral enhancement in lesion on the left.

B, T1-weighted MR images (TR 600 msec, TE 25 msec) show multiple central foci of high intensity with surrounding hypointensity. Some central foci are also partially isointense. This case is notable for the multiplicity of cryptic vascular malformations.

C and D, On proton density and T2-weighted MR images (TR 2000 msec, TE 35/70 msec), characteristic isointensity or hyperintensity in the center is surrounded by extensive peripheral hypointensity. Some foci that were hyperintense on T1-weighted image have become hypointense or isointense on current images (arrows); others have remained hyperintense (arrowheads). The discrepancy is most likely due to a predominance of intracellular hemoglobin breakdown products in the former case, as compared with free compounds in the latter case, in these evolving hemorrhages. In addition, the powerful T2 relaxation effects of hemosiderin from previous bleeds obscure smaller foci of higher signal on second echo of long TR sequence.

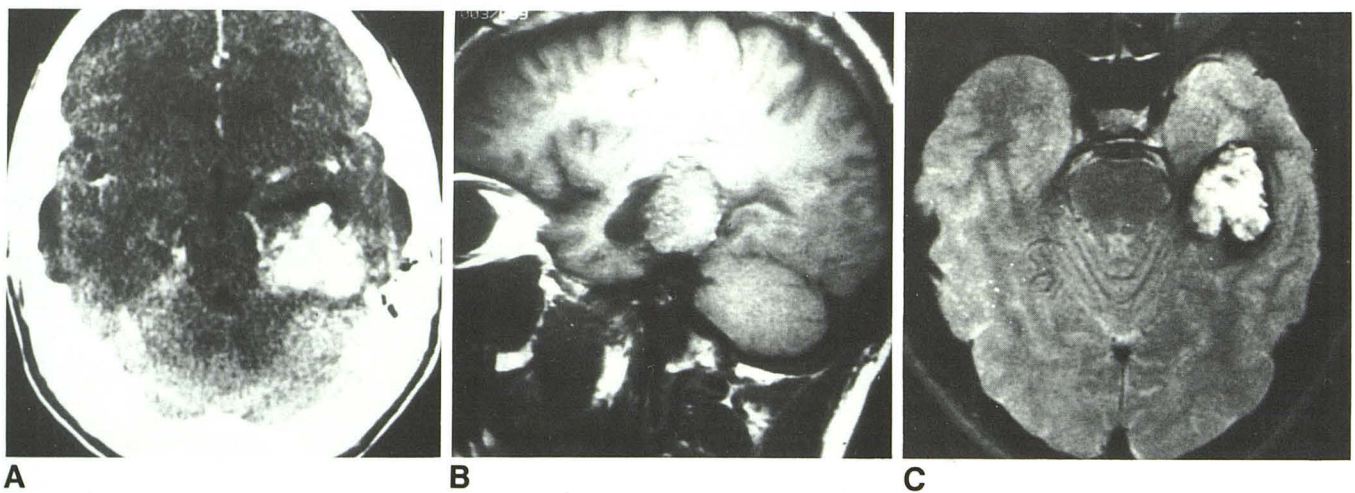


Fig. 3.—34-year-old man with seizure disorder. Surgical pathology: cryptic vascular malformation.

A, Contrast-enhanced CT scan shows large enhancing mass with primarily intraventricular location and trapping of distal temporal horn.

B, T1-weighted sagittal MR images (TR 600 msec, TE 25 msec) confirm intraventricular location of mass. In addition, the mass is primarily isointense, with a few foci of increased signal.

C, T2-weighted MR images (TR 2000 msec, TE 70 msec) now show lesion to be of high signal, with scattered areas of lesser signal. In addition, a prominent hypointense rim surrounds lesion, creating an appearance most consistent with the paramagnetic effect of hemosiderin.

hypointense (Fig. 2). In addition, surrounding these regions was peripheral low signal, which became even more hypointense on the second echo of the long TR sequence. One case appeared as a single punctate hypointensity on both T1- and T2-weighted images. Two of the six cases showed mild edema surrounding the lesions. Pathology revealed thrombosed vascular malformations in the five surgically proven cases. In one case, changes most consistent with cavernous hemangioma were demonstrated. In another case, probable arteriovenous malformation was noted. In the remaining cases, the exact pathologic categorization of the vascular malformation could not be made. All the vascular malformations exhibited regions of acute and chronic hemorrhage in the matrix of abnormal vascular tissue. Hemosiderin deposition of varying degrees was seen in all lesions.

#### *Hemorrhagic Neoplasms*

Of the 18 cases with hemorrhagic neoplasms, three consisted of primary tumors—an astrocytoma, an oligodendroglioma, and a meningioma. Both gliomas showed typical CT characteristics of mild hypodensity with irregular enhancement. Heavy punctate calcification was present in the oligodendroglioma. The meningioma, likewise, was not unusual in CT appearance with multiple foci of calcification and homogeneous enhancement. Two of the lesions lacked substantial mass effect; the third was associated with mild edema. Despite the conventional appearance of these lesions on CT, all these tumors displayed unusual MR characteristics, with striking similarity in their appearance to the occult vascular malformations noted above (Fig. 4).

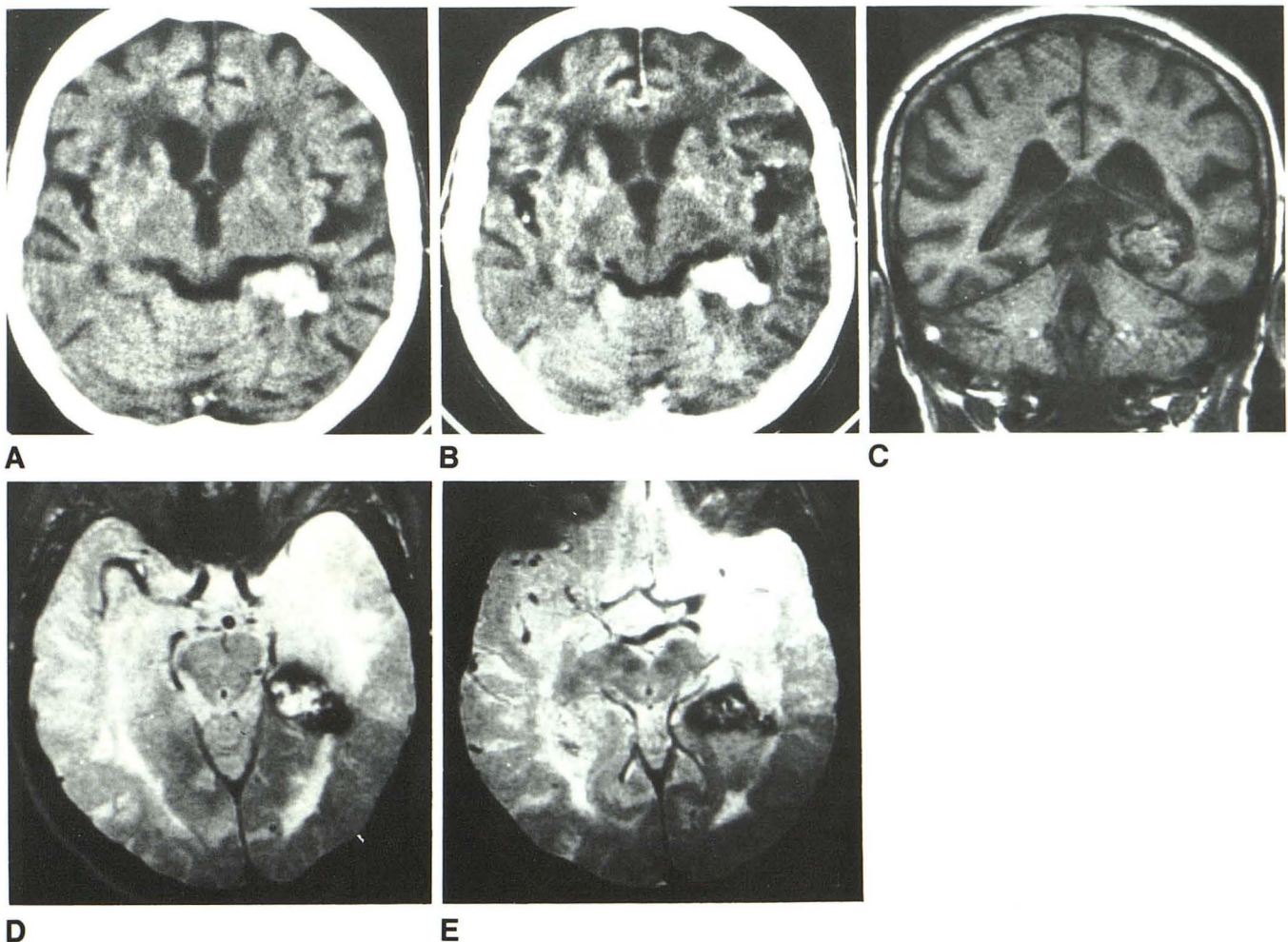


**Fig. 4.**—72-year-old woman with a headache. Surgical pathology: hemorrhagic meningioma.

**A and B,** CT scans with and without contrast show highly calcified lesion extending inferiorly from choroid plexus. Enhancement after contrast is present.

**C,** T1-weighted MR images (TR 500 msec, TE 25 msec) confirm presence of lesion. It is primarily isointense, although there are small foci of high signal within it.

**D and E,** T2-weighted MR images (TR 2000, TE 70 msec) show a mass with high-intensity signal and surrounding rim of low-intensity signal. While portions of low-intensity rim may be due to calcification, a portion of the low intensity is most likely due to hemosiderin deposition as well. Marked hemosiderin stains were observed at pathology. Note striking resemblance of this case to Fig. 3, both in the lesion's appearance and in its lack of mass effect.

The 15 remaining cases were composed of hemorrhagic metastasis and contained a total of 42 lesions visible on MR. The number of lesions per case varied from one to 14, with an average of nearly three. CT scans without and with contrast were positive in 13 of 15 cases. In two cases, multiple punctate metastases clearly visible on MR were missed by CT. In the 13 positive scans, CT missed additional lesions in two cases. In all positive cases, lesions were variable in density on noncontrast CT scans. In one of the 15 patients, the lesion appeared hypodense. In two of the 15, the lesions appeared to have a low-density center surrounded by a slightly hyperdense ring. In three of the 15, the lesions were isodense, and in another six patients, focal hyperdensity was seen. In the remaining patient, different lesions were both isodense and hyperdense. No calcification was seen in any of the lesions. Contrast enhancement was generally present. Larger lesions were usually associated with considerable surrounding edema, but smaller lesions often did not display significant mass effect.

MR scans were positive in all cases and showed hemorrhagic metastasis in greater number and generally more prominently than did CT scans. On T1-weighted images, areas of high central signal were seen in 10 of the 15 scans. In five cases, only isointense signal was noted centrally. In two

cases, some lesions contained central foci of both high signal and isointense signal. Surrounding hypointensity was seen in 12 of the 15 cases on T1-weighted images. T2-weighted images uniformly showed lesions with isointense or highly intense central signal surrounded by peripheral hypointensity. In 12 of 15 cases, the lesions were surrounded by edema. However, in three cases, all with multiple punctate lesions, no surrounding edema was seen (Fig. 5).

In all of the surgically resected hemorrhagic neoplasms, distinctive tumor, often with associated clot, was visible in the pathologic sections. The yellow-brown stains typical of hemosiderin deposition were present in all cases and very prominent in five of the 10 cases.

### Discussion

By MR criteria, both cryptic vascular malformations and hemorrhagic neoplasms may appear similar. In the former, the MR findings have been attributed to the evolution of extravascular intracerebral blood [2]. Our pathology results, with evidence of blood and hemosiderin deposition, suggest that identical mechanisms are operative in hemorrhagic neoplasms.

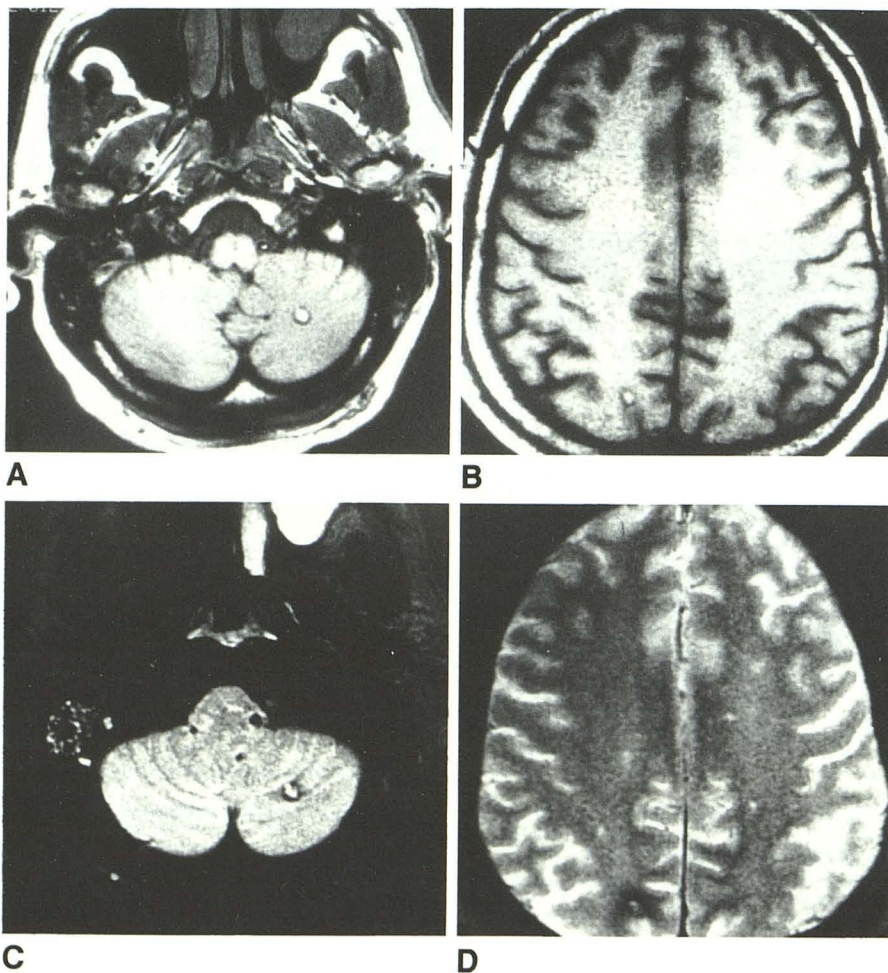


Fig. 5.—43-year-old man with extensive metastatic choriocarcinoma. Clinical diagnosis: metastatic choriocarcinoma.

A and B, T1-weighted MR images (TR 600 msec, TE 20 msec) show several foci of high signal with low-intensity rims. Other sections revealed several more lesions.

C and D, T2-weighted MR scans (TR 2000 msec, TE 70 msec) again show foci of hyperintensity surrounded by more extensive rings of hypointensity. These lesions are remarkably similar to those of Fig. 1, both in their appearance and in their lack of edema.

The central foci of high signal most likely represent subacute to chronic hemorrhage and are presumed to be caused by paramagnetic methemoglobin [7], which shortens T1 relaxation times substantially and can slightly shorten T2 relaxation times as well. If the central focus is hyperintense on both short and long TR sequences, as is most often the case, then the methemoglobin is considered to be homogeneously distributed and free in solution after red blood cell lysis (Fig. 2). However, if the central focus is hyperintense on T1-weighted images and hypointense on T2-weighted images, then the hemoglobin breakdown products are still primarily intracellular. Again, the paramagnetic methemoglobin contributes to shortening of the T1 relaxation time, while the remaining deoxyhemoglobin that has not yet been oxidized to methemoglobin causes a magnetic susceptibility effect and preferential T2 relaxation by virtue of its heterogeneous distribution within the intact red blood cells.

The cause of the isointensity of the central core of some lesions on T1-weighted images is unclear and can be seen with both cryptic vascular malformations and hemorrhagic neoplasms (Figs. 3B and 4C). It may be secondary to chronicity of the bleed and the long-term appearance of an organized hematoma. Alternatively, it may be due to recent hemorrhage prior to evolution to a more intense phase. Acute (as opposed to hyperacute) hematomas appear isointense or slightly hypointense on short TR sequences. Finally, the isointense central core may represent abnormal vasculature in the case of occult vascular malformation or tumor matrix in the case of hemorrhagic neoplasm. Therefore, while foci of adjacent nonhemorrhagic tumor may be seen in larger neoplasms, nodular areas without the high signal of subacute blood are also present in occult vascular malformations. On T1-weighted images, both can appear isointense and virtually identical. The corresponding T2-weighted images can appear

hypointense or isointense, if evolving hemorrhage is involved, or even hyperintense, if abnormal vasculature, organized thrombus, or tumor are present (Figs. 3C, 4D, and 4E).

The surrounding hypointensity is thought to be consistent with a preferential T2 relaxation effect from the deposition of paramagnetic hemosiderin in macrophages [7]. Thus, the peripheral dark rim becomes even more prominent and hypointense on the second echo of the long TR sequence (Fig. 6). Some hypointensity is also due to calcification in certain cases [8] (Fig. 1).

Because the underlying mechanisms responsible for producing the characteristic MR findings in all of our patients are primarily those of the evolution of hemorrhage, it is likely that other subacute to chronic hemorrhagic lesions, such as the occasional infectious foci that bleed, may also appear identical in some cases. We have observed a case of chronic fungal abscess, which displayed MR characteristics consistent with paramagnetic effect and was revealed to have heavy hemosiderin deposition at surgery.

The similarity on MR of hemorrhagic neoplasm and occult vascular malformation raises the problem of differentiating between the two, an obviously crucial issue. Clinically, both entities often present with nonspecific symptoms. Headache, seizures, and waxing and waning neurologic deficits may be seen in both, although a clinical course of years makes occult vascular malformation more likely [9]. Even cerebral metastasis may present subacutely, with headache the initial symptom in the majority of cases [9]. Although most of the patients with hemorrhagic metastasis who were referred to us already had known systemic metastasis, this fact is primarily due to the nature of the Memorial Sloan-Kettering Cancer Center as a tertiary referral center. Since occasional patients with malignancies initially present with brain metastasis, the finding of a lesion otherwise typical of the occult

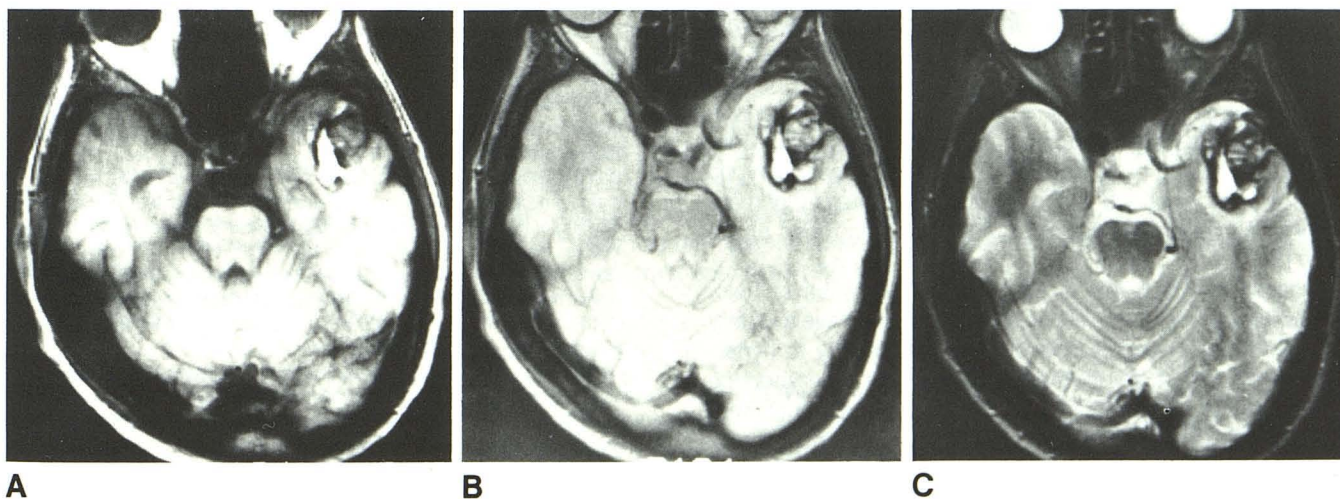


**Fig. 6.**—66-year-old man with melanoma. Surgical pathology: metastatic melanoma. The metastasis was hemorrhagic and virtually amelanotic. **A**, T1-weighted images (TR 600 msec, TE 20 msec) show lesion of mixed isointensity and hyperintensity centrally, with surrounding hypointensity. The lesion has an appearance similar to that described as typical for cryptic vascular malformations. **B** and **C**, Proton density and T2-weighted MR images (TR 2000 msec, TE 35/70 msec) again show a lesion similar to that in Fig. 5. Central core remains either isointense or hyperintense, and peripheral hypointensity has increased. Although there is a minimal amount of surrounding edema and mass effect, these features can also be seen in cryptic vascular malformations.

vascular malformation may actually be the first indication of a systemic malignancy.

In our series, size and location were not of help in differentiating cryptic vascular malformation from hemorrhagic neoplasm. Both ranged in size from punctate to large and both occurred in nonspecific locations, although cryptic vascular malformation and metastasis exhibited a preference for the gray-white junction [9, 10]. Perhaps, a brainstem location is more typical of cryptic malformation [11], but metastasis [9] and, of course, primary glioma can certainly occur there as well.

Despite the similarity on MR between cryptic vascular malformation and hemorrhagic neoplasm, several criteria appear to be of help in differentiating these entities:

1. Neoplasms are often noted for prominent surrounding edema. In our series, a metastasis over  $\frac{1}{2}$  cm was almost uniformly associated with edema. In some cases, the edema was extensive. In contrast, edema surrounding the cryptic vascular malformations was unusual, and, if present, was almost always mild. The extent of edema certainly helps to differentiate many of the larger metastases from cryptic vascular malformations on MR, even when the appearance is otherwise identical. However, previous reports suggest that up to 50% of cryptic vascular malformations may be associated with some edema [12]. Conversely, an occasional metastasis is associated with little edema (Fig. 6), especially if the patient is on steroids. In addition, punctate metastasis often displays no evidence of surrounding edema. Furthermore, two of the three primary tumors in our series lacked edema. In these cases, differentiation from small cryptic vascular malformation is virtually impossible.

2. Some of the malignancies that often lead to hemorrhagic metastasis, such as melanoma, are prone to exhibit a multiplicity of lesions [9]. Clearly, the average number of lesions in the cases of hemorrhagic metastasis (3) exceeded the average number of cryptic vascular malformations (1.5) in our patients. However, gliomas and other primary cerebral neoplasms are generally single. In addition, although cryptic vascular malformations are often single, recent reports have suggested that up to 50% cases may actually contain multiple lesions [10] (Fig. 2). Therefore, the multiplicity of lesions is helpful in suggesting metastasis but again not specific. Conversely, the finding of a single lesion may be typical of cryptic vascular malformations but may also characterize primary tumors and certain metastatic tumors, such as those of the colon [9].

In cases in which MR is equivocal, CT may be of help. Hemorrhagic neoplasms, especially metastasis, have a variety of appearances, ranging from cystlike low density to hyperdensity. In contrast, cryptic malformations tend to be isodense or hyperdense on noncontrast CT, with some enhancement after administration of contrast [11, 12]. Other appearances, such as low density [3] or ring lesions [4], have been noted and were present in one case in our study but are unusual.

CT may also be useful in defining calcification, since its presence is highly unusual in untreated cerebral metastasis. Calcification is seen in a minority of cases of cryptic vascular

malformation (Fig. 1). Previous papers note an occurrence of definite granular calcification ranging from 20–33% [1, 3, 4, 10]. Our findings are consistent with these figures. However, calcification may also be present in gliomas and meningiomas. Thus, if the lesion displays calcification on the noncontrast CT scan, hemorrhagic metastasis but not primary tumor can be virtually excluded. The absence of calcification cannot be used to suggest the etiology.

In conclusion, MR lesions often referred to as "typical" of occult vascular malformation may actually represent neoplasm. Multiplicity and the presence of adjacent edema, especially if extensive, suggest a neoplastic origin. However, even if small and single, these lesions must not be dismissed as occult vascular malformation, and an underlying neoplasm must be considered. In questionable cases, CT may provide further information. Since both primary and secondary hemorrhagic neoplasm can appear identical to cryptic vascular malformation, the MR finding of the "typical occult vascular malformation" should now at least merit consideration of an underlying neoplasm and further evaluation or follow-up.

#### ACKNOWLEDGMENTS

We thank Patricia Dudley for help in manuscript preparation and Bruce Peters, Nicole Baccon, and Noreen O'Donnell for technological assistance.

#### REFERENCES

1. Kucharczyk W, Lemme-Plegos L, Uske A, Brant-Zawadzki M, Dooms GC, Norman D. Intracranial vascular malformations: MR and CT imaging. *Radiology* **1985**;156: 383–389
2. Gomori J, Grossman R, Goldberg H, Hackney DB, Zimmerman RA, Bilaniuk LT. Occult cerebral vascular malformations: high-field MR imaging. *Radiology* **1986**;158: 707–713
3. Lemme-Plegos L, Kucharczyk W, Brant-Zawadzki M, et al. MR imaging of angiographically occult vascular malformations. *AJNR* **1986**;7: 217–222
4. New P, Ojemann R, Davis K, et al. MR and CT of occult vascular malformations of the brain. *AJNR* **1986**;7: 771–779, *AJR* **1986**;147: 985–993
5. Heier LA, Amster JL, Zimmerman RD, et al. Focal recurrent hemorrhage on MR at 0.5 T—an aid to the diagnosis of cryptic cerebral vascular malformations. Presented at the XIIIth Symposium Neuroradiologicum, Stockholm, Sweden, June **1986**. *Acta Radiol [Suppl] (Stockh) (in press)*
6. Griffin C, De La Paz R, Enzmann D. Magnetic resonance imaging of brainstem cryptic arteriovenous malformation. Presented at the annual meeting of the Western Neurological Society, Monterey, CA, October **1985**
7. Gomori J, Grossman R, Goldberg H, Zimmerman RA, Bilaniuk LT. Intracranial hematomas: Imaging by high-field MR. *Radiology* **1985**;157: 87–93
8. Oot R, New P, Pile-Spellman J, et al. The detection of intracranial calcifications by MR. *AJNR* **1986**;7: 801–809
9. Galich J, Sundaresan N. Metastatic brain tumors. In: Wilkins H, Rengachary S, eds. *Neurosurgery*. New York: McGraw-Hill, **1985**: 597–610
10. Patel SC, Sanders WP, Fuentes J, Haggag A, Mehta B, Boulous R. Angiographically occult vascular malformation of the brain: MR imaging at 1.5 Tesla. Presented at the 72nd annual meeting of the Radiological Society of North America, Chicago, November **1986**
11. Yeates A, Enzmann D. Cryptic vascular malformations involving the brainstem. *Radiology* **1983**;146: 71–75
12. Kramer R, Wing S. Computed tomography of angiographically occult cerebral vascular malformations. *Radiology* **1977**;123: 649–652